

Metal nanoparticle/carbon quantum dot composite as photocatalyst for high efficiency cyclohexane oxidation

Ruihua Liu, Hui Huang, Haitao Li, Yang Liu, Jun Zhong, Youyong Li, Shuo Zhang, and Zhenhui Kang

ACS Catal., Just Accepted Manuscript • Publication Date (Web): 11 Dec 2013

Downloaded from <http://pubs.acs.org> on December 12, 2013

Just Accepted

"Just Accepted" manuscripts have been peer-reviewed and accepted for publication. They are posted online prior to technical editing, formatting for publication and author proofing. The American Chemical Society provides "Just Accepted" as a free service to the research community to expedite the dissemination of scientific material as soon as possible after acceptance. "Just Accepted" manuscripts appear in full in PDF format accompanied by an HTML abstract. "Just Accepted" manuscripts have been fully peer reviewed, but should not be considered the official version of record. They are accessible to all readers and citable by the Digital Object Identifier (DOI®). "Just Accepted" is an optional service offered to authors. Therefore, the "Just Accepted" Web site may not include all articles that will be published in the journal. After a manuscript is technically edited and formatted, it will be removed from the "Just Accepted" Web site and published as an ASAP article. Note that technical editing may introduce minor changes to the manuscript text and/or graphics which could affect content, and all legal disclaimers and ethical guidelines that apply to the journal pertain. ACS cannot be held responsible for errors or consequences arising from the use of information contained in these "Just Accepted" manuscripts.



ACS Publications
High quality. High impact.

ACS Catalysis is published by the American Chemical Society, 1155 Sixteenth Street N.W., Washington, DC 20036

Published by American Chemical Society. Copyright © American Chemical Society. However, no copyright claim is made to original U.S. Government works, or works produced by employees of any Commonwealth realm Crown government in the course of their duties.

Metal nanoparticle/carbon quantum dot composite as photocatalyst for high efficiency cyclohexane oxidation

Ruihua Liu,¹ Hui Huang,¹ Haitao Li,¹ Yang Liu,^{*1} Jun Zhong,¹ Youyong Li,¹ Shuo Zhang,² and Zhenhui Kang^{*1}

¹*Institute of Functional Nano and Soft Materials (FUNSOM) & Jiangsu Key Laboratory for Carbon-Based Functional Materials and Devices, Soochow University, Suzhou, China. E-mail: yangl@suda.edu.cn; zhkang@suda.edu.cn.*

²*Shanghai Synchrotron Radiation Facility, Shanghai Institute of Applied Physics, Chinese Academy of Science, Shanghai, China*

KEYWORDS: carbon quantum dots, composites, cyclohexane oxidation, photocatalysis; selective oxidation

ABSTRACT

High-efficiency and high-selectivity catalytic oxidation of alkanes under mild conditions is a major aim of current catalysis chemistry and chemical production. Despite extensive development efforts on new catalysts for cyclohexane oxidation, current commercial processes still suffer from low conversion, poor selectivity, and excessive production of wastes. We

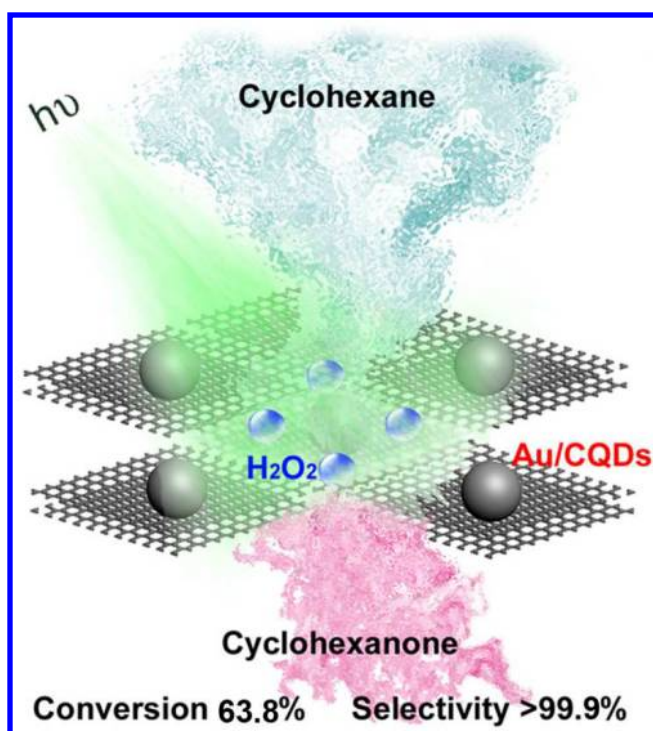
demonstrate the design and synthesis of metal nanoparticles/carbon quantum dots (CQDs) composites for high-efficiency and high-selectivity photocatalyst systems for the green oxidation of cyclohexane. Remarkably, the present Au nanoparticles/CQDs composite photocatalyst yields 63.8% conversion efficiency and 99.9% selectivity for green oxidation of cyclohexane to cyclohexanone using H_2O_2 under visible light at room temperature. Given its diversity and versatility of structural and composition design, metal nanoparticles/CQDs composites may provide a powerful pathway for the development of high-performance catalysts and production processes for green chemical industry.

INTRODUCTION

One of the principal aims of catalysis chemistry in the 21st Century is high-efficiency and high-selectivity catalytic oxidation of alkanes,¹ especially cyclohexane oxidation under mild conditions.² However, the high activation energy of C-H bond breaking in cyclohexane dictates harsh reaction conditions, i.e. high temperature and high pressure.³ Apart from its intrinsic importance in the chemistry of C-H activation, the selective oxidation of cyclohexane to cyclohexanone and cyclohexanol (about 10^6 tons per year) is the key step of the commercial production of nylon-6 and nylon-66 polymers. Despite extensive development efforts for cyclohexane oxidization catalysts, today's commercial processes still suffer from high temperature (150–160 °C), high pressure (1–2 MPa), low yield (< 15%), low selectivity (< 80%), and excessive production of wastes.^{4,5} Catalysts enabling cyclohexane oxidation under mild conditions (below the boiling point of cyclohexane, 80.7 °C) would alleviate the potential hazard of harsh reaction conditions, as well as allow for more selective and controlled reactions. As a preferred oxidant in liquid phase, hydrogen peroxide can work at low temperature, produces only water as a by-product and has a high oxygen uptake (47%).^{6–8} However, cyclohexane oxidation

with H_2O_2 at low temperature using the current catalysts (such as weak acid resin,⁹ iron bispidine complexes,¹⁰ Ru complex,¹¹ Cr/Ti/Si oxides,¹² Na-GeX,¹³ mesoporous TS-1,¹⁴ Ti-MCM-41,¹⁵ metal aluminophosphates,¹⁶ biomimetic systems¹⁷ and Cu- Cr_2O_3 ¹⁸) invariably suffers from large amount of organic solvent (i.e. acetone and acetonitrile), poor selectivity, and low H_2O_2 efficiency, thus making its industrialization difficult.

Scheme 1. Au/CQDs composites as a photocatalyst for selective oxidation of cyclohexane in the presence of H_2O_2 under visible light.



Carbon quantum dots (CQDs) with richly fluorescent and photo-electrochemical properties^{19,20} can serve as either photo-induced electron acceptors or donors.²⁰ They can function not only as an efficient photocatalyst (for highly selective oxidation), but also as a multi-functional component in photocatalyst design²¹ to promote wider spectrum absorption and separation of electron-hole, as well as to stabilize photolysis semiconductors. Metal nanoparticles (Au, Cu, etc.)

are known to possess catalytic activities for selective oxidation reactions.^{22,23} Additionally, surface plasma resonance absorption can also induce good photocatalytic abilities of metal nanoparticles (Au, Ag, etc.).^{24,25} Here, we report the design of a tunable photocatalyst based on the composite of CQDs and metal nanoparticles for the selective oxidation of cyclohexane. Significantly, the Au nanoparticles/CQDs (Au/CQDs) composite catalyst yielded oxidation of cyclohexane to cyclohexanone with 63.8% efficiency and >99.9% selectivity in the presence of H₂O₂ under visible light at room temperature (see Scheme 1).

Results and discussion

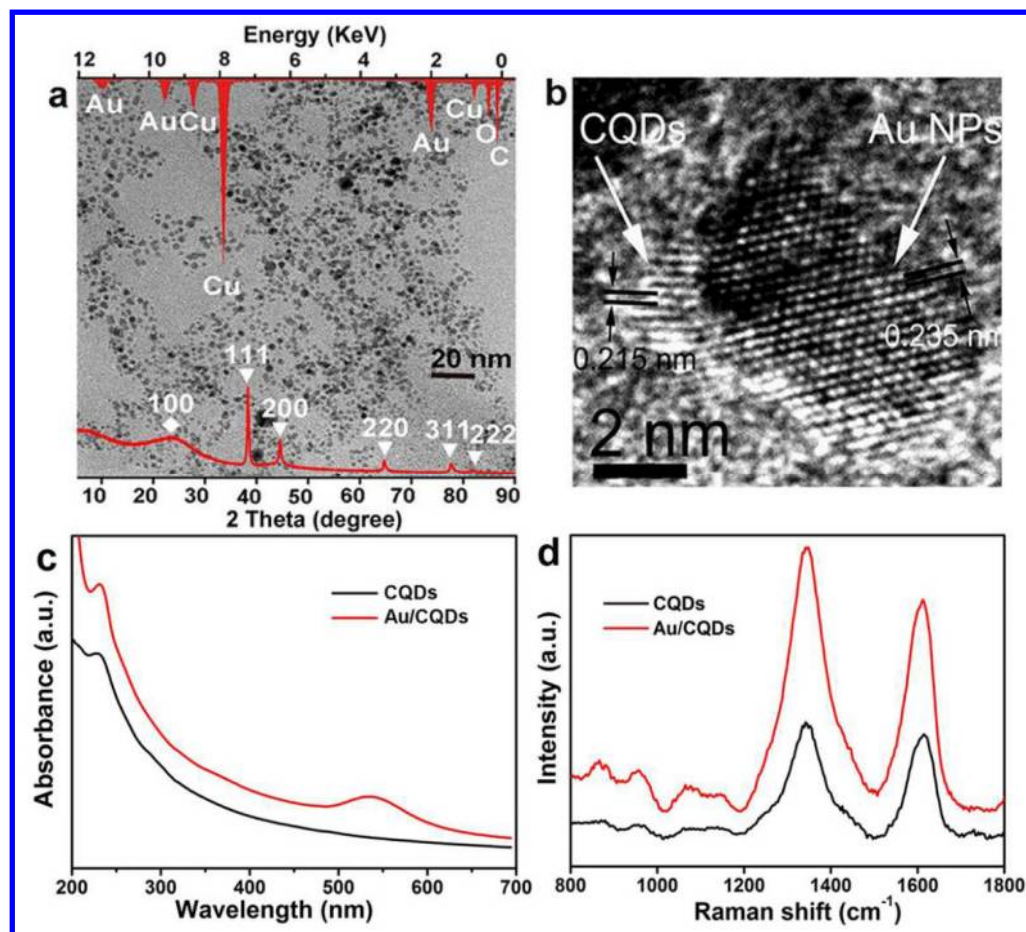


Figure 1. (a) TEM image, X-ray diffraction (XRD) pattern (inset, upper of 1a) and energy dispersive X-ray (EDX) spectrum (inset, lower of 1a) of Au/CQDs composites; (b) HRTEM image of Au/CQDs composites; (c) The UV-vis absorbance spectrum of CQDs and Au/CQDs; (d) Typical Raman spectra of CQDs and Au/CQDs composites.

Characterization of Au/CQDs composites. The CQDs were synthesized through a method of electrochemical ablation of graphite. As shown in Figure S1, the surface functional groups on the CQDs are hydroxyl (-OH), carboxy (C=O), and epoxide/ether (C-O-C). For the present composite catalyst, the interaction between the p/π orbits of C and d orbits of Au in AuNPs, and the interactions between the functional groups on the CQDs (-OH, C=C, C=O) and the AuNPs are responsible for the formation and the high stability of the Au/CQDs composite catalyst. Au/CQDs composites were synthesized by drop-wise addition of HAuCl₄ solution to CQDs solution with vigorously magnetic stirring in dark at room temperature (see Experimental section for details). Figure 1a shows the transmission electron microscopy (TEM) image of the spherical and well-dispersed Au/CQDs composites with sizes of 5-15 nm. The upper inset in Figure 1a is the energy dispersive X-ray (EDX) spectrum of Au/CQDs composites, where the copper peaks are from the copper TEM grid, gold peaks from AuNPs, oxygen and carbon peaks from CQDs and amorphous carbon film in Cu grid. X-ray diffraction (XRD) pattern is shown in the lower inset in Figure 1a. All the characteristic diffraction peaks marked by “ ” can be readily indexed to (111), (200), (220), (311) and (222) planes of metallic Au (JCPDS No. 1-1172), respectively. The broad diffraction peak at 26° (marked by “◇”) is the characteristic peak of carbon. The high-resolution TEM image (HRTEM) of Au/CQDs composites is shown in Figure 1b. Clear lattice spacing's of 0.240 nm and 0.235 nm are in well agreement with the (100) crystallographic planes of graphitic carbon and (111) planes of crystalline Au, respectively. Compared with that of

CQDs or AuNPs, the UV-Visible absorption spectrum of Au/CQDs composites displays typical absorbance in both UV and visible regions. In Figure 1c, the absorption peak at about 230 nm represents a typical absorption of CQDs, similar to that of polycyclic aromatic hydrocarbons,²⁶ while the absorption peak in the visible region (490 to 590 nm) is attributed to the surface plasmon band of AuNPs.²⁷ The Raman spectrum of Au/CQDs composites in Figure 1d shows the D-band and G-band of carbon at 1343 and 1611 cm^{-1} .²⁸ The intensity of D-band and G-band of Au/CQDs composite is obviously higher than that of pure CQDs, which is due to the surface enhancement Raman scattering effect of AuNPs.²⁹

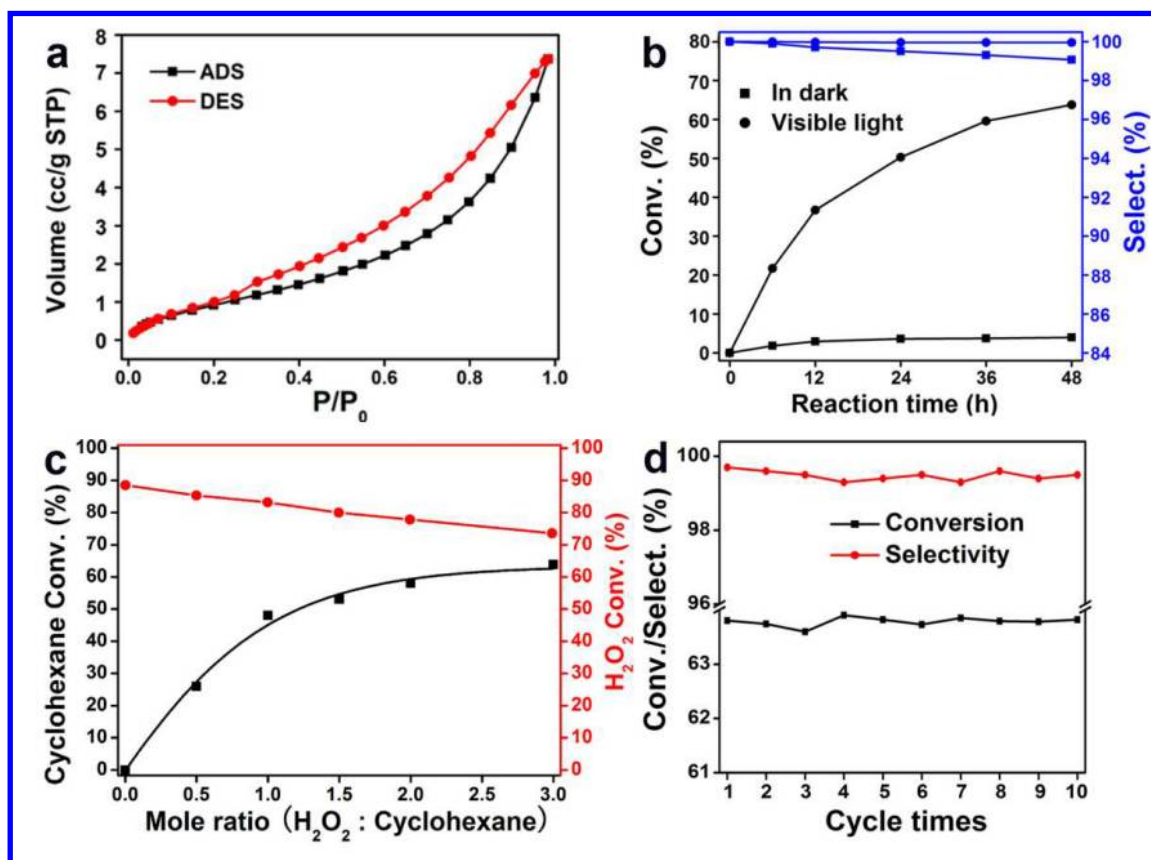


Figure 2. (a) Cyclohexane adsorption-desorption isotherm curves of Au/CQDs composites;(b) Time dependence of conversion efficiency and selectivity of cyclohexane oxidation were investigated under dark and visible light (mole ratio of H_2O_2 /cyclohexane is 3:1); (c) The

conversion of cyclohexane and H_2O_2 under different mole ratios of $\text{H}_2\text{O}_2/\text{cyclohexane}$; (d) Conversion and selectivity efficiency of the oxidation of cyclohexane on Au/CQDs composites over cycling ten times (mole ratio of $\text{H}_2\text{O}_2/\text{cyclohexane}$, 3:1).

Catalytic oxidation of cyclohexane using Au/CQDs composites. The measured cyclohexane adsorption-desorption isotherm of Au/CQDs composites (Figure 2a) exhibits the type-IV curve characteristics,³⁰ indicating that Au/CQDs composites have good adsorption to cyclohexane. In the catalytic experiments, H_2O_2 (30%) as oxidant was added dropwise to the mixture of Au/CQDs composites (25 mg) and cyclohexane (50 mL) in a round bottom flask (250 mL) with water condenser and continuous magnetic stirring. The oxidation products were analyzed by gas chromatography (GC) and gas chromatography-mass spectroscopy (GC-MS). Figure 2b shows the time dependence of the conversion and selectivity of cyclohexane oxidation to cyclohexanone with Au/CQDs composites as the photocatalyst driven by visible light. It reveals that conversion efficiency increases with increasing reaction time, while the selectivity to cyclohexanone is nearly constant at 99.9% regardless of the conversion efficiency (Table 1). After 48 h reaction, a high conversion efficiency of 63.8% and high selectivity of over 99.9% were achieved concurrently. The conversion of cyclohexane and H_2O_2 under different mole ratios of $\text{H}_2\text{O}_2/\text{cyclohexane}$ (0.0, 0.5, 1.0, 1.5, 2.0, 3.0) were also investigated and shown in Figure 2c. With the mole ratio of $\text{H}_2\text{O}_2/\text{cyclohexane}$ increasing, the conversion of cyclohexane increases and the conversion of H_2O_2 slightly decreases.

The following experiments further highlight the effectiveness of the present composite catalyst: (1) Blank reaction (i.e., without catalyst) would not produce any oxidation products (entry 1, Table 1); (2) CQDs and AuNPs used separately as catalyst (entries 2 and 3, Table 1) yielded cyclohexane oxidation with low conversion of only 3% and 5%, respectively; and (3) A

mixture of CQDs and AuNPs as catalyst yielded slight improvement, but conversion and selectivity of cyclohexane to cyclohexanone remained low at 7.0% and 76.5%, respectively (entry 4, Table 1). In remarkable contrast, the Au/CQDs composites catalyst shows high conversion efficiency (63.8%) and high selectivity (> 99.9%), which also remain nearly constant over ten catalytic cycles (Figure 2d). After carefully analyzing the products, it was found that the selectivity of C₆ products is about 100% (see Table 1), without any CO₂ evolved. As shown in Figure 2d, the Au/CQDs are stable enough during the repeated experiments without exhibiting any significant loss of catalytic activity and selectivity. After recycling ten times, Au/CQDs still retain high catalytic activity and selectivity of cyclohexane oxidation. Moreover, the filtrate solution test (additional 24 h reaction after removing the Au/CQDs composites from the reaction medium) showed no catalytic activity, indicating leaching did not play an important role in the present system. The above experiments show Au/CQDs composites indeed function as a high-performance photocatalyst in the present reaction system.

Table 1. Different catalysts for photocatalytic oxidation of cyclohexane (mole ratio of H₂O₂/cyclohexane is 3:1).

Entry	Catalyst	Oxidant	Conversion	Selectivity	Selectivity
			(%)	(%)	(%)
				cyclohexanone	$\sum_{\text{sel}} C_6$
1	None	None	-	-	-
2	CQDs	H ₂ O ₂	3.0	99.9	100

3	AuNPs	H ₂ O ₂	5.0	98.4	100
4	CQDs &AuNPs	H ₂ O ₂	7.0	76.5	100
5	Au/CQDs	H ₂ O ₂	63.8	> 99.9	100
6	Au/SiO ₂	H ₂ O ₂	30.3	54.1	100
7	Au/Carbon nanotube	H ₂ O ₂	22.1	49.7	100
8	Au/Graphene	H ₂ O ₂	23.9	50.1	100
9	Au/Graphite	H ₂ O ₂	14.2	64.2	100

Reactions were carried out in a round bottom flask (see Methods information for details). Conversion and selectivity were determined by GC analysis; the variance of values is estimated to be less than $\pm 2\%$.

Cyclohexane oxidation was further carried out with the Au/CQDs composites catalyst driven by light of different wavelengths (Figure 3a). Figure 3b shows that the best conversion efficiency was obtained in green light, whose wavelength matches the surface plasma resonance zone of AuNPs (490-590 nm, see Figure S2).²⁷ However, under the same conditions (visible light, room temperature), the use of AuNPs supported on SiO₂ spheres (Au/SiO₂ nanospheres; TEM and HRTEM images, see Supporting information Figure S3) as catalyst only yielded a low conversion efficiency of 30.3% and low selectivity of 54.1% for cyclohexanone (entry 6, Table 1). While, other carbon based catalysts (such as Au/Carbon nanotubes, Au/graphite, and Au/Graphene) also could not get good photocatalytic abilities on the cyclohexane oxidation (entries 7, 8 and 9 Table 1). The totality of the experiments shows that the high conversion and selectivity in the present photocatalyst system should be attributed to the collective contribution and interactions of CQDs and AuNPs.

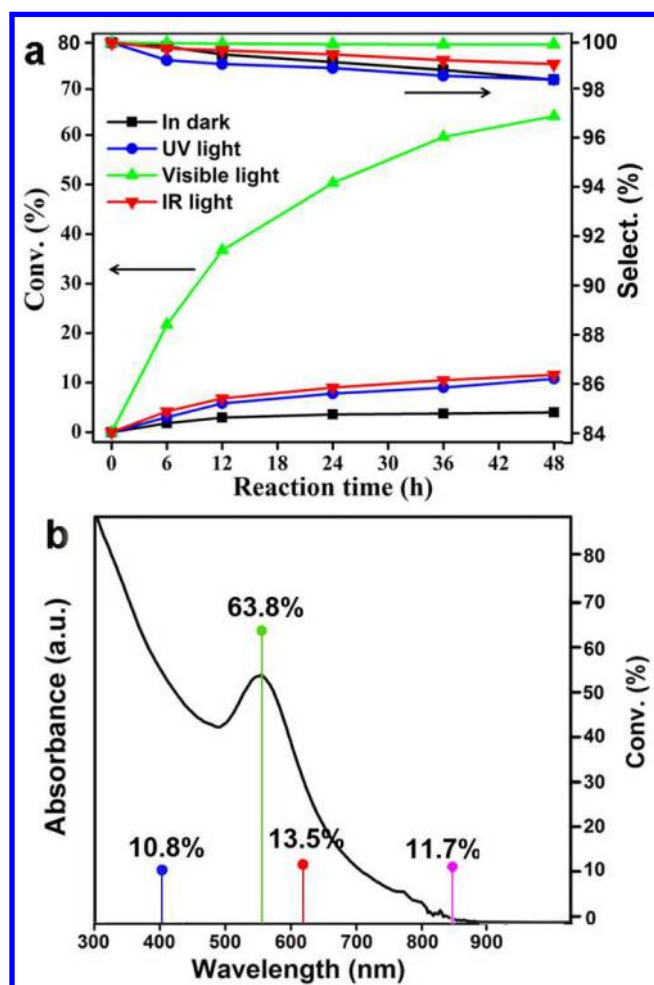


Figure 3. Time dependence of the conversion and selectivity of the oxidation of cyclohexane with Au/CQDs composites as photocatalyst (mole ratio of H_2O_2 /cyclohexane is 3:1) driven by different lighting conditions: (a) under dark, UV light (high pressure mercury lamp, main wavelength 365 nm), Visible light (Xe lamp with visible-CUT filter to cut off light of wavelength < 420 nm), and IR light (Xe lamp with visible-CUT filter to cut off light of wavelength < 700 nm); (b) blue (400 nm), green (525 nm), red (620 nm), and IR (850 nm) light, using high power (>1 W) LED as light source.

Interaction between AuNPs and CQDs. X-ray absorption spectroscopy (XAS, element-specific spectroscopic technique for structural information of different species) experiments were performed to investigate the electronic structure of Au/CQDs composites.³¹ Au L_3 -edge (X-ray absorption near edge structure, XANES) and (Extended x-ray absorption fine structure, EXAFS) data for Au/CQDs composites with and without visible light irradiation were collected. The XANES data are shown in Figure 4a and the Fourier transform of the EXAFS data in R space shown in Figure 5a. The XANES data for Au/CQDs composites with and without visible light irradiation also show very similar spectral shape. In contrast, obvious differences between light-on and -off can be found in the Fourier transform of the EXAFS data in the R space. The main peak around 2.6 Å can be attributed to Au-Au bonds. Au/CQDs composites before light irradiation show a main peak at 2.6 Å indicating the existence of AuNPs, and the peak intensity is lower than that for Au foil revealing the nature of AuNPs.³² Strikingly, when the same Au/CQDs composites were exposed to visible light, a new peak at 1.5 Å can be observed. This peak could be attributed to the interaction between CQDs and AuNPs, such as Au-C bonds.³² Also, a further decrease of the main peak intensity can be observed, suggesting decrease of Au-Au bonds with formation of Au-C bonds. In followed the experiments, Au L_3 -edge XANES and EXAFS data for Au/CQDs composites were collected during the in situ photocatalytic reaction. Under the in situ reaction condition, the XANES data for Au/CQDs composites (Figure 4b) is also very similar to that for Au NPs and Au foil. While, as shown in Figure 5b, under the in situ reaction condition, there is no obvious signal on the formation of Au-C bonds between CQDs and AuNPs, even if a further decrease of the main peak (2.6 Å) intensity can be observed under visible light. The disappearing of the Au-C bonds signal further confirms that the photocatalytic reaction is really occurred on the interface of AuNPs and the CQDs.

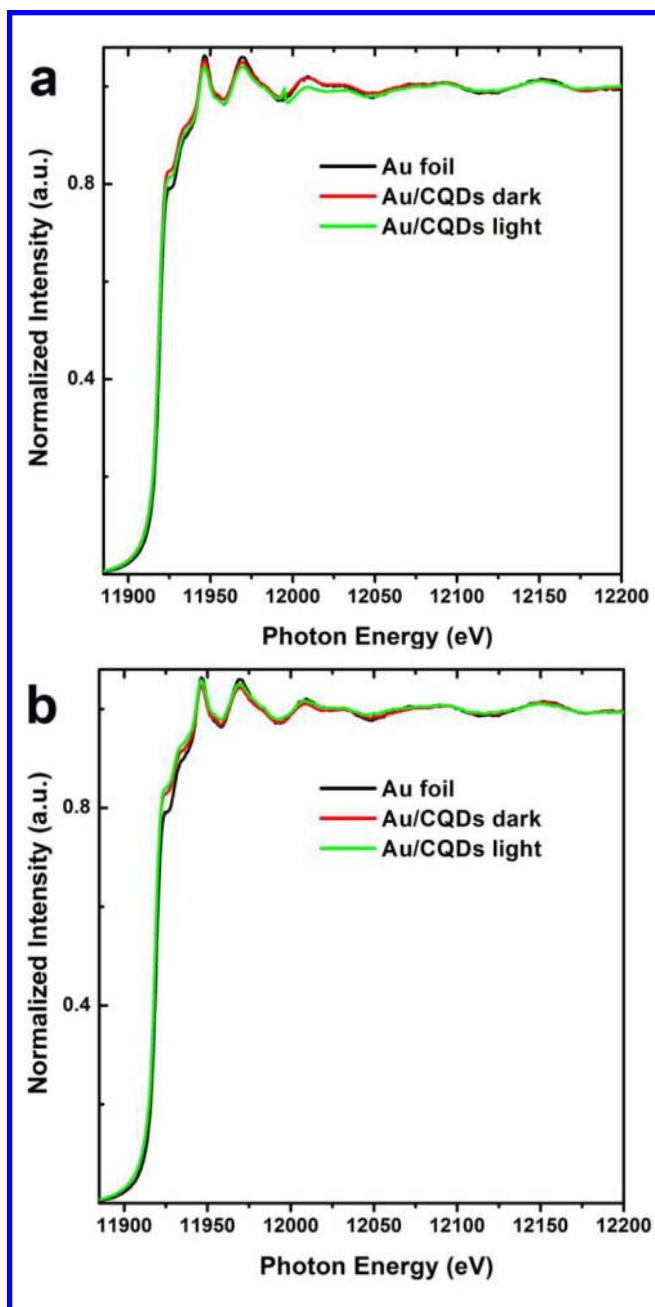


Figure 4. (a) Au L_3 -edge XANES spectra of Au/CQDs composites with and without visible light irradiation. (b) Au L_3 -edge XANES spectra of Au/CQDs composites with and without visible light irradiation under in situ reaction condition.

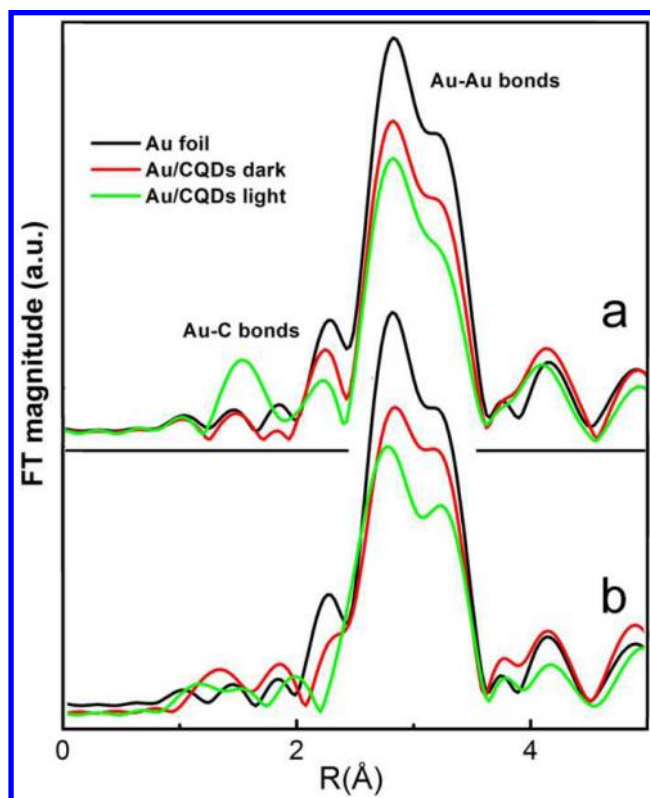


Figure 5. (a) The Fourier transform of the Au/CQDs composites EXAFS data in R space with and without light. (b) The Fourier transform of the Au/CQDs composites EXAFS data in R space with and without light under in situ reaction condition. The spectrum of Au foil is also shown for comparison.

In the followed experiments, the photo-induced electron transfer properties of CQDs irradiated by visible light were investigated. It was found that the photoluminescence (PL) of CQDs excited by 485 nm with emission located at 550 nm could be quenched by either electron acceptor or electron donor molecules in solution, confirming that CQDs are excellent as both electron donors and acceptors under visible light. As shown in Figure S4a and S4b, CQDs can exhibit broad luminescence peak at about 550 nm with the excitation at 485 nm, and the emission intensities were quenched by the known electron donors N, N-diethylaniline (DEA) and electron acceptors 2, 4-dinitrotoluene. Figure S4c and S4d show the luminescence decays of

13

CQDs with Stern-Volmer quenching constants (insets of Figure S4c and S4d, $K_{sv} = \tau_F^0 k_q$) from linear regression of 33.0 and 21.5 M^{-1} , respectively. The above results that the PL of CQDs were quenched highly efficiently by either electron acceptors or electron donors, clearly confirming that CQDs are excellent as both electron acceptors and electron donors.

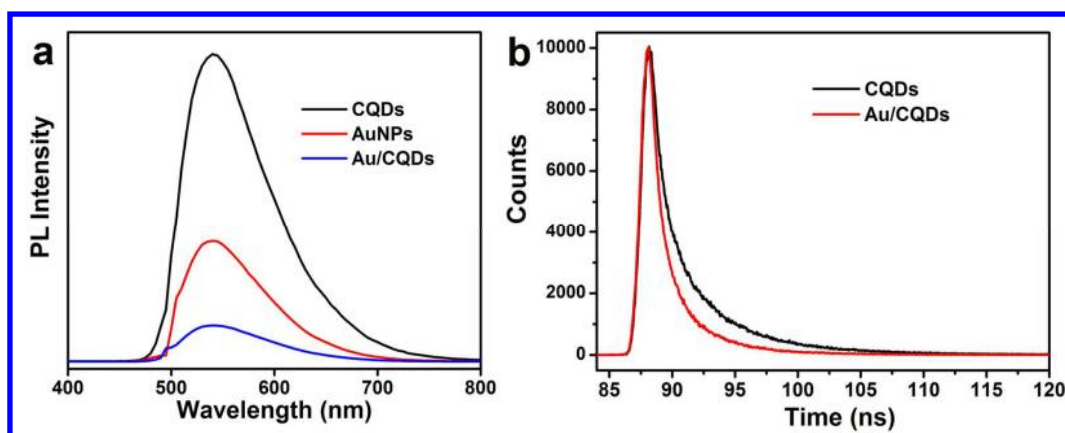


Figure 6. (a) PL spectra (485 nm excitation) of CQDs, AuNPs and Au/CQDs; (b) Luminescence decays (485 nm excitation, monitored with 550 nm narrow bandpass filter) of CQDs and Au/CQDs.

To obtain the further insight about the interaction between AuNPs and CQDs, we examined the PL spectra of CQDs, AuNPs, and Au/CQDs (Figure 6a). It indicated that the PL of CQDs is effectively quenched in the Au/CQDs system. The corresponding PL life time of Au/CQDs shown in Figure 6b decreased to 1.5 ns, from 4.0 ns for pure aqueous CQDs solution. It demonstrates the dynamic PL quenching in the Au/CQDs system is attributed to an ultrafast electron transfer process in the Au/CQDs system.

Proposed mechanism study. The electrocatalytic ability of Au/CQDs composites for H_2O_2 decomposition was examined in a conventional three-electrode electrochemical cell.²⁰ As shown in Figure 7a the bare glassy carbon electrode shows no obvious electrochemical response (black

curve), while Au/CQDs-modified glassy carbon electrode exhibits obvious catalytic ability for H_2O_2 decomposition. Under visible light irradiation, the response of Au/CQDs-modified electrode for H_2O_2 decomposition is stronger (onset potential at -0.2 V) than that without light irradiation (onset potential at -0.6 V). Further experiments show that Au/CQDs composites-modified electrodes have the highest electrocatalytic activity for H_2O_2 decomposition among various modified electrodes (CQDs, AuNPs and their mixture), which is also consistent with the photocatalytic results in Table 1. All electrochemical experiments suggested that the visible light-promoted catalytic activity of Au/CQDs composites for H_2O_2 decomposition should play key roles for the highly catalytic activity in selective oxidation of cyclohexane.

In general, $\text{HO}\cdot$ produced by decomposition of H_2O_2 is a strong oxidant, and can easily oxidize cyclohexane into cyclohexanone and cyclohexanol. Here, a spin-trapping electron spin resonance (ESR) test was carried out to check the active oxygen species produced by Au/CQDs- H_2O_2 system under visible light. As shown in Figure 7b, typical characteristic quartet peaks of $\text{DMPO}\cdot\text{OH}$ (DMPO , dimethyl pyridine N-oxide) adducts appeared gradually upon light irradiation of the aqueous Au/CQDs- H_2O_2 system, which suggested that $\text{HO}\cdot$ is the active oxygen species in this photocatalytic oxidation process. To further confirm whether $\text{HO}\cdot$ is the main active oxygen specie responsible for present selective oxidative reaction, a terephthalic acid PL (TA-PL) probing assay was used to detect the amount of $\text{HO}\cdot$ under different reaction conditions³³ (see Experimental section). The reaction between the hydroxyl radicals and terephthalate yielding one intensely fluorescent monohydroxylated isomer is shown in Figure S5. Figure 7c confirms that in the buffer solution containing Au/CQDs catalyst, a larger number of $\text{HO}\cdot$ will be produced under visible light irradiation than that for in dark.

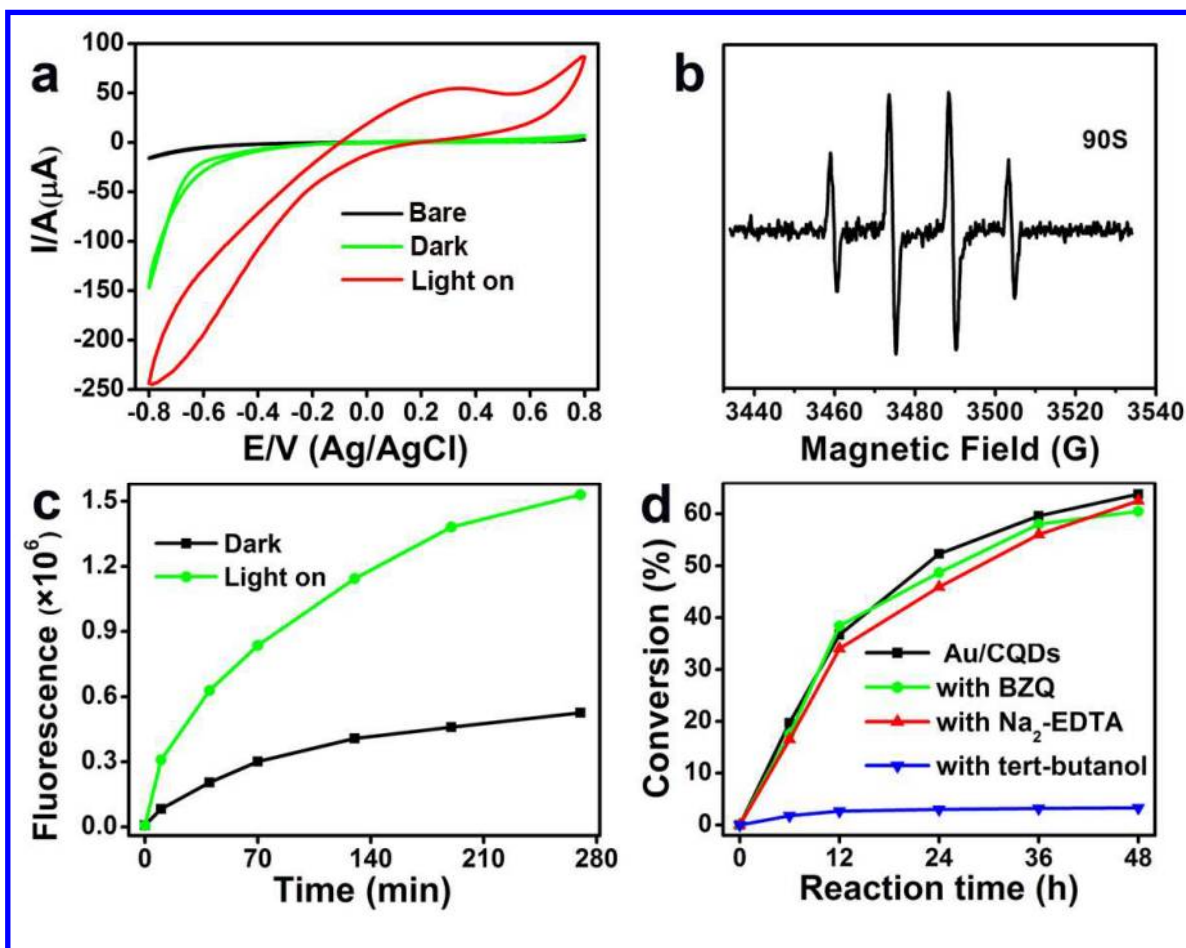


Figure 7. (a) Cyclic voltammograms of bare glassy carbon electrode and Au/CQDs-modified glassy carbon electrode in phosphate buffer (PH = 7.4) and in the presence of 10 mM H_2O_2 . Scan rate, 25 mV/s. A 450 W Xe lamp was used as light source with visible-CUT filter to cut off light of wavelength < 420 nm; (b) The ESR signals of the DMPO-•OH (aqueous solution) adducts for Au/CQDs- H_2O_2 system under visible light irradiation. $[\text{Au/CQDs}] = 4$ mg/50 mL; $[\text{H}_2\text{O}_2] = 10$ mM; $[\text{DMPO}] = 40$ mM; (c) Time dependence of the fluorescence intensity of the supernatant liquid of Au/CQDs composites for two different reaction conditions (in dark and under visible light). A 450 W Xe lamp was used as light source with visible-CUT filter to cut off light of wavelength < 420 nm; (d) Photocatalysis activities of Au/CQDs in reactive species trapping

experiments with three kinds of reactive species scavengers (mole ratio of H₂O₂/cyclohexane, 3:1).

Figure 8 shows the PL intensities of the supernatant TA-PL assay solutions after removing the Au/CQDs composites with or without visible light irradiation, and the result suggested that a higher amount of HO· was generated by the irradiated sample than that by the non-irradiated one. In the followed control experiments, to further confirm the active oxygen species with radical characteristics, toluene was selected as the substrate in the following experiments. After 12 h reaction, methyl group-oxygenated compounds (benzyl alcohol, benzaldehyde, benzoic acid, etc.) were produced in high selectivity of > 92%, whereas a mixture of cresols (o- : m- : p- isomer ratio = 2.6 : 0.8 : 5.7) was only produced in small amounts (selectivity less than 8 % summing the three). Generally speaking, the methyl group oxygenation requires abstraction of an H· radical by active oxygen species with radical characteristics.^{34,35} The further reactive species trapping experiments were carried out with three different scavengers, *tert*-butanol (a ·OH radical scavenger), benzquinamide (BZQ, a O²⁻· radical scavenger) and disodium ethylenediaminetetraacetate (Na₂-EDTA, a hole scavenger). Figure 7d shows the photocatalytic results after addition of three different scavengers. The addition of *tert*-butanol substantially reduced the photocatalytic activity for the oxidation of cyclohexane from almost 63.8% to 3.3% after 48 h reaction, while the introduction of BZQ and Na₂-EDTA barely affect the photocatalysis results. All of above experiments confirm that that HO· is the active oxygen species in this photocatalytic oxidation process.

In our present photocatalytic system, as discussed above, the reaction happened in the interface between Au NPs and CQDs. Although the hydroxy radicals have strong oxidation abilities, the

synergic effect of the functions of CQDs and the SPR (surface plasmonic resonance) of AuNPs, still can protect the products (cyclohexanone and cyclohexanol) from the over oxidation.

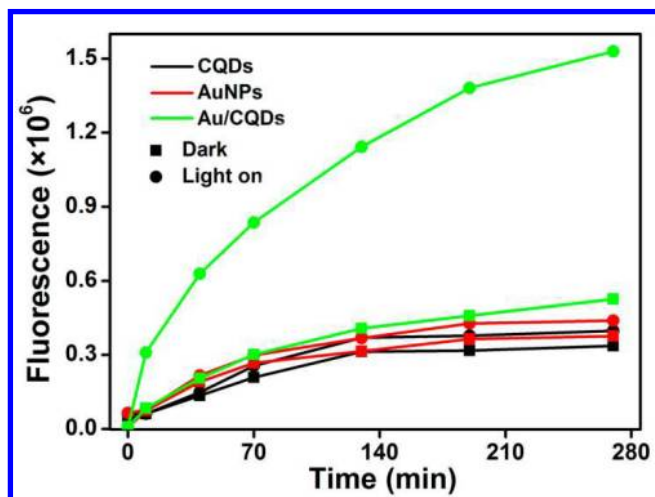


Figure 8. Time dependence of the fluorescence intensity of the supernatant liquid of CQDs, AuNPs, and Au/CQDs composites for two different reaction conditions (in dark and under visible light). A 450 W Xe lamp was used as light source with visible-CUT filter to cut off light of wavelength < 420 nm.

Tunable-design ability of metal/CQDs photocatalysts system. The totality of the experiment results suggests the following mechanistic processes in the photocatalytic oxidation of cyclohexane. The surface plasma resonance of AuNPs enhances the light absorption of Au/CQDs composites. Under visible light, H_2O_2 is decomposed to hydroxyl radical ($\text{HO}\cdot$), which serves as a strong oxidant for conversion of cyclohexane to cyclohexanone. In the process, the interaction between CQDs and AuNPs under visible light plays a key role in the eventual high conversion and selectivity. Based on the proposed mechanism, Ag nanoparticles/CQDs (Ag/CQDs) (see Supporting information Figure S6) and Cu nanoparticles/CQDs (Cu/CQDs) composite photocatalysts (see Supporting information Figure S7) were synthesized, and used to

catalyze cyclohexane oxidation under the same condition with Au/CQDs system. Like the Au/CQDs system, Ag/CQDs and Cu/CQDs composites exhibited similarly good catalytic performance (see Supporting information Table S1 and Table S2) under purple light (conversion 54.0%, selectivity 84.1% for Ag) and red light (conversion 46.7%, selectivity 75.3% for Cu), which correspond respectively to the surface plasma resonance of Ag (see Supporting information Figure S6b) and Cu (see Supporting information Figure S7b) nanoparticles. The results were consistent with the proposed catalytic mechanism discussed above. It is therefore possible to tune the wavelength response of the present photocatalyst system based on the surface plasma resonance of metal nanoparticles to achieve high-efficiency and high-selectivity oxidation of cyclohexane, as shown in Figure 9.

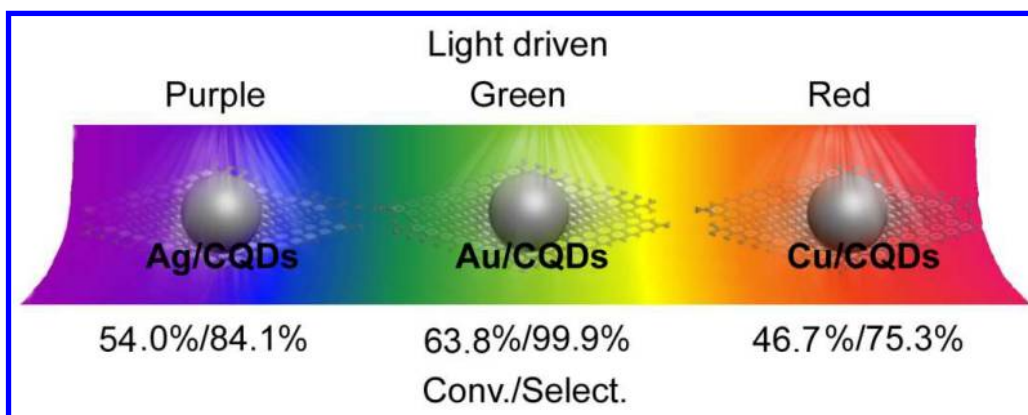


Figure 9. Based on the surface plasma resonance of metal nanoparticles, Ag/CQDs, Au/CQDs and Cu/CQDs are catalytically active under purple, green and red light, respectively.

EXPERIMENTAL SECTION

General information. Unless otherwise noted, all materials including dry solvents were obtained from commercial suppliers and used without further purification. All chemicals were purchased from Sigma–Aldrich. Transmission electron microscopy (TEM) images were recorded

using a FEI/ Philips Techal 12 BioTWIN TEM operated at 200 kV with EDX analyses. HRTEM images were obtained with a CM200 FEG TEM. UV-visible spectra were measured with an Agilent 8453 UV-VIS Diode Array Spectrophotometer, while the PL study was conducted with a Horiba Jobin Yvon (FluoroMax 4) Luminescence Spectrometer. We also collected Raman spectra on an HR 800 Raman spectroscopy (J Y, France) equipped with a synapse CCD detector and a confocal Olympus microscope. The spectrograph used 600 g mm⁻¹ gratings and a 633 nm He-Ne laser. The crystal structure of the resultant products was characterized by X-ray powder diffraction (XRD) by using an 8/ X'Pert-ProMPD (Holand) D/max-γAX-ray diffractometer with Cu Kα radiation ($\lambda=0.154178$ nm). The GC were performed in a Varian 3400 GC column with a cross-linked 5% PhMe silicone column (25 m × 0.20 mm × 0.33 μm) and a FID detector under the following conditions: carrier gas (N₂) at 140 K; temperature program 60 °C, 1 min, 15 °C /min, 180 °C, 15 min; split ratio, 6 : 1; injector, 280 °C; detector, 280 °C. X-ray Absorption Near Edge Structure (XANES) and Extended X-ray Absorption Fine Structure (EXAFS) data were collected on beamline 14W at the Shanghai Synchrotron Radiation Facility. The electrocatalysis action of CQDs was tested by a CHI 660C workstation (CH Instruments, Chenhua, Shanghai, China), while the fluorescence lifetimes of the CQDs were measured by FluoroLog 3-211-TCSPC.

General Procedure for Preparation of CQDs. The CQDs were synthesized through a method of electrochemical ablation of graphite. In the synthetic process, two identical graphite rods placed parallel (99.99%, Alfa Aesar Co. Ltd., 13 cm in length and 0.6 cm in diameter) were inserted into the electrolyte at 3 cm above the liquid surface and used as both cathode and anode in a separation distance of 7.5 cm. The electrolyte was ultrapure water (18.4 MΩ cm⁻¹, 600 mL) without any other additives. Static potentials of 15–60 V were applied to the two electrodes using

a direct current (DC) power supply for ten days with intense stirring. Subsequently, a dark-yellow solution appeared gradually in the reactor. The solution was filtered with slow-speed quantitative filter paper, and the resultant solution was centrifuged at 22000 rpm for 30 min to remove the precipitated graphite oxide and graphite particles. Finally, the obtained solution contained water soluble CQDs.

General Procedure for Preparation of AuNPs. AuNPs were prepared by chemical reduction method. A aqueous solution (20 mL) containing HAuCl_4 ($2.5 \times 10^{-4} \text{ mol}\cdot\text{L}^{-1}$) and trisodium citrate ($2.5 \times 10^{-4} \text{ mol}\cdot\text{L}^{-1}$) were prepared in a conical flask under continuous vigorous stirring. Then ice-cold freshly NaBH_4 solution (0.6 mL, $0.1 \text{ mol}\cdot\text{L}^{-1}$) was added into the above solution. The resultant solution turned pink immediately after adding NaBH_4 , indicating the formation of AuNPs.

General Procedure for Preparation of Au/CQDs Composites. The Au/CQDs composite was obtained by dropwise addition of HAuCl_4 solution (400 μL , $25 \text{ mmol}\cdot\text{L}^{-1}$) to CQDs solution (20 mL) with vigorous magnetic stirring in dark environment at room temperature. The resultant mixture was under constant magnetic stirring at room temperature for 2 h, aged overnight, the solution turned red, implying the Au/CQDs composites were obtained. Then, the Au/CQDs composites were centrifuged at 12000 rpm for 15 min, washed three times with deionized water and ethanol respectively, and finally the obtained sample were dried 6 h at 25-60°C.

Photo-induced electron transfer properties of CQDs. The PL and photo-induced electron transfer properties of CQDs irradiated by visible light were investigated. In this experiment, PL spectra of the CQDs in organic solutions were recorded with luminescence emission intensities (485 nm excitation, laser source), which were quenched by the known electron acceptors 2,4-

dinitrotoluene and electron donors N,N-diethylaniline in toluene solution (different concentration). The Stern–Volmer quenching constants ($K_{SV} = \tau_F^0 k_q$) were obtained from linear regression. The luminescence decays were tested by TCSPC method. For the CQDs sample, when the excitation wavelength is 485 nm, we monitored the sample with 550 nm narrow bandpass filter, with the observed Stern–Volmer quenching constants ($K_{SV} = \tau_F^0 k_q$) from linear regression.

The Electrocatalytic Activity of Au/CQDs Composites. The electrocatalytic activity of Au/CQDs composites for H_2O_2 decomposition was tested in a conventional three-electrode electrochemical cell with a platinum wire as the auxiliary electrode and an Ag/AgCl (saturated KCl) as the reference electrode. The working electrodes were Au/CQDs composites-modified glassy carbon electrode. The Au/CQDs composites-modified glassy carbon electrode was prepared by spreading aqueous Au/CQDs composites over glassy carbon electrode. A 450 W Xe lamp was used as light source with visible-CUT filter to cut off light of wavelength < 420 nm to get visible light, and was positioned 3 cm away from the photoelectrochemical cell. The cyclic voltammograms (CVs) of the bare glassy carbon electrode and Au/CQDs composites over glassy carbon electrode were obtained in 0.05 M phosphate buffer solution (PBS, pH 7.4) in the presence of different H_2O_2 concentration at a scan rate of 25 mV/s. The photocurrent signal was recorded with a CHI 660C workstation (CH Instruments, Chenhua, Shanghai, China) connected to a personal computer. All electrochemical experiments were carried out at room temperature.

Terephthalic Acid Photoluminescence Probing Assay (TA–PL) to Detect the $HO\bullet$. Terephthalic acid (THA, 0.415 g), sodium phosphate (Na_3PO_4 , 2.2 g), and deionizer water were added into 250 mL volumetric flask to form a buffer at pH 7.5. After adding a suitable amount of

catalyst into the buffer, the mixture was irradiated by visible light or no light. Product fluorescence (THA-OH) was measured with a fluorescent spectrophotometry (Horiba Jobin Yvon, FluoroMax 4) with 350 nm excitation and 429 nm emission at pH 7.5.

CONCLUSIONS

In conclusion, we report that, the Au/CQDs composite shows unprecedentedly high photocatalytic activity for the selective oxidation of cyclohexane to cyclohexanone with conversion efficiency of 63.8% and selectivity of over 99.9% using H₂O₂ as oxidant without any solvents. The mechanism of the catalyst system is proposed to involve: enhancement of light absorption by surface plasma resonance of metal nanoparticles, production of active oxygen species (HO·) by H₂O₂ decomposition, and interaction between CQDs and AuNPs under visible light; these processes collectively lead to the eventual high conversion and selectivity. The present work suggests a new route for the design of high-performance photocatalytic systems for selective hydrocarbon oxidation for green chemical industry.

ASSOCIATED CONTENT

Supporting Information., UV-vis spectra and (HR)TEM images of metal nanoparticles/CQDs composites. This material is available free of charge via the Internet at <http://pubs.acs.org>.

AUTHOR INFORMATION

Corresponding Author

* E-mail: zhkang@suda.edu.cn; yangl@suda.edu.cn.

ACKNOWLEDGMENT

This work is supported by the National Basic Research Program of China (973 Program) (2012CB825800, 2013CB932702), the National Natural Science Foundation of China (51132006, 21073127, 21071104), the Specialized Research Fund for the Doctoral Program of Higher Education (20123201110018), a Suzhou Planning Project of Science and Technology (ZXG2012028), a Foundation for the Author of National Excellent Doctoral Dissertation of China (200929), and a project funded by the Priority Academic Program Development of Jiansu Higher Education Institutions.

REFERENCES

- (1) Schuchardt, U.; Cardoso, D.; Sercheli, R.; Pereira, R.; da Cruz, R. S.; Guerreiro, M. C.; Mandelli, D. ; Spinacé, E. V.; Pires, E. L. *Appl. Catal. A* **2001**, 211, 1-17.
- (2) Cao, Y. H.; Yu, H.; Tan, J.; Peng, F.; Wang, H. J.; Li, J.; Zheng, W. X.; Wong, N.-B. *Carbon* **2013**, 57, 433-442.
- (3) Bromberg, S. E.; Yang, H.; Asplund, M. C.; Lian, T.; McNamara, B. K.; Kotz, K. T.; Yeston, J. S.; Wilkens, M.; Frei, H.; Bergman, R. G.; Harris, C. B. *Science* **1997**, 278, 260-263.
- (4) Hattori, H.; Ide, Y.; Ogo, S.; Inumaru, K.; Sadakane, M.; Sano, T. *ACS Catal.* **2012**, 2, 1910-1915.
- (5) Wang, C. H.; Chen L. F.; Qi, Z. W.; *Catal. Sci. Technol.* **2013**, 3, 1123-1128.
- (6) Bonnet, D.; Ireland, T.; Fache, E.; Simonato, J.-P. *Green Chem.* **2006**, 8, 556-559.

- (7) Hamdy, M. S.; Ramanathan, A.; Maschmeyer, T.; Hanefeld, U.; Jansen, J. C. *Chem. Eur. J.* **2006**, 12, 1782-1789.
- (8) Pillai, U.; Sahle-Demessie, R. E. *Chem. Commun.* **2002**, 0, 2142-2143.
- (9) Chavez, F. A.; Nguyen, C. V.; Olmstead, M. M.; Mascharak, P. K. *Inorg. Chem.* **1996**, 35, 6282-6291.
- (10) Comba, P.; Maurer, M.; Vadivelu, P. *Inorg. Chem.* **2009**, 48, 10389-10396.
- (11) Goldstein, A. S.; Beer, R. H.; Drago, R. S. *J. Am. Chem. Soc.* **1994**, 116, 2424-2429.
- (12) Yiu, S.-M.; Man, W.-L.; Lau, T.-C. *J. Am. Chem. Soc.* **2008**, 130, 10821-10827.
- (13) Pârvulescu, V. I.; Dumitriu D.; Poncelet, G. *Catal. A-Chem.* **1999**, 140, 91-105.
- (14) Spinacé, E. V.; Pastore, H. O.; Schuchardt, U.; *J. Catal.* **1995**, 157, 631-635.
- (15) Lü, G. M.; Ji, D.; Qian, G.; Qi, Y. X.; Wang, X. L.; Suo, J. S. *Appl. Catal. A* **2005**, 280, 175-180.
- (16) Raja, R.; Sankar, G.; Thomas, J. M. *J. Am. Chem. Soc.* **1999**, 121, 11926-11927.
- (17) Yuan, Y.; Ji, H. B.; Chen, Y. X.; Han, Y.; Song, X. F.; She, Y. B.; Zhong, R. G. *Org. Process Res. Dev.* **2004**, 8, 418-420.
- (18) Sarkar, B.; Prajapati, P.; Tiwari, R.; Tiwari, R.; Ghosh, S.; Acharyya, S. S.; Pendem, C.; Singha, R. K.; Konathala, L. N. S.; Kumar, J.; Sasaki, T.; Bal, R. *Green Chem.* **2012**, 14, 2600-2606.

- (19) Baker, S. N.; Baker, G. A. *Angew. Chem. Int. Ed.* **2010**, 49, 6726-6744.
- (20) Li, H. T.; Liu, R. H.; Lian, S. Y.; Liu, Y.; Huang, H.; Kang, Z. H. *Nanoscale* **2013**, 5, 3289-3297.
- (21) Li, H. T.; He, X. D.; Kang, Z. H.; Huang, H.; Liu, Y.; Liu, J. L.; Lian, S. Y.; Tsang, C. H. A.; He, X. D.; Lee, S.-T. *Angew. Chem. Int. Ed.* **2010**, 49, 4430-4434.
- (22) Wittstock, A.; Zielasek, V.; Biener, J.; Friend, C. M.; Bäumer, M.; *Science* **2010**, 327, 319-322.
- (23) Gu, J. L.; Gu, Y. L.; Huang, Y.; Elangovan, S. P.; Li, Y. S.; Zhao, W. R.; Toshio, I.; Yamazaki, Y.; Shi, J. L. *J. Phys. Chem. C* **2011**, 115, 21211-21217.
- (24) Shimizu, K.-I.; Murata, Y.; Satsuma, A. *J. Phys. Chem. C* **2007**, 111, 19043-19051.
- (25) Shankar, S. S.; Rai, A.; Ahmad, A.; Sastry, M. *J. Colloid Interf. Sci.* **2004**, 275, 496-502.
- (26) Li, H. T.; Kang, Z. H.; Liu, Y.; Lee, S.-T. *J. Mater. Chem.* **2012**, 22, 24230-24253.
- (27) Baruah, B.; Craighead, C.; Abolarin, C. *Langmuir* **2012**, 28, 15168-15176.
- (28) Ming, H.; Ma, Z.; Liu, Y.; Pan, K. M.; Yu, H.; Wang, F.; Kang, Z. H. *Dalton Trans.* **2012**, 41, 9526-9531.
- (29) Luo, P. H.; Li, C.; Shi, G. Q. *Phys. Chem. Chem. Phys.* **2012**, 14, 7360-7366.
- (30) Li, J.; Shi, Y.; Xu, L.; Lu, G. Z. *Ind. Eng. Chem. Res.* **2010**, 49, 5392-5399.
- (31) Jiang, D. T.; Sham, T. K.; Norton, P. R. *Phys. Rev. B* **1994**, 49, 3709-3712.

1
2
3
4
5
6
7
8
9
10
11
12
13
14
15
16
17
18
19
20
21
22
23
24
25
26
27
28
29
30
31
32
33
34
35
36
37
38
39
40
41
42
43
44
45
46
47
48
49
50
51
52
53
54
55
56
57
58
59
60

(32) Zhang, P.; Sham, T. K. *Phys. Rev. Lett.* **2003**, 90, 245502.

(33) Miyake, T.; Hamada, M.; Sasaki, Y.; Oguri, M. *Appl. Catal. A* **1995**, 131, 33-42.

(34) Kang, Z. H.; Wang, N. B.; Mao, B. D.; Su, Z. M.; Gao, L.; Niu, L.; Shan, H. Y.; Xu, L. *Appl. Catal. A* **2006**, 299, 212-217.

(35) Niwa, S.-I.; Eswaramoorthy, M.; Nair, J.; Raj, A.; Itoh, N.; Shoji, H.; Namba T.; Mizukami, F. *Science* **2002**, 295, 105-107.